Synthesis, Solid State Structures, and Properties of Linear and Tripodal Flexible Molecules with Pyrazinopyrazine Moieties

Yuto Ohmura, Ryusei Oketani, Akihito Konishi[2], Makoto Yasuda[2], and Ichiro Hisaki[1,*]

[1] Division of Chemistry, Graduate School of Engineering Science, Osaka University, 1-3 Machikaneyama, Toyonaka, Osaka 560-8531
[2] Department of Applied Chemistry, Graduate School of Engineering, Osaka University, Suita, Osaka 565-0871
**Corresponding author:* Division of Chemistry, Graduate School of Engineering Science, Osaka University, 1-3 Machikaneyama, Toyonaka, Osaka 560-8531. *Email: i.hisaki.es@osaka-u.ac.jp*

Abstract

Pyrazino[2,3-*b*]pyrazine (PP), which is a naphthalene analogue with iminium nitrogen atoms at 1,4,5,8-positions instead of sp^2-carbon atoms, is attractive as a building block for nitrogen-highly-contained π-conjugated systems. In this study, we synthesized PP-based linear and tripodal molecules, in which PP moieties are bonded with the central benzene ring at 1,4-positions and 1,3,5-positions, respectively, giving conformationally flexible and moderately π-conjugated molecules. It is noteworthy that the tripodal one forms unique interdigitated dimer with a small cavity in a crystalline state because of flexible tripodal molecular shape.

Keywords: pyrazinopyrazine, heterocyclic compound, flexibility, crystal engineering

Graphical abstract

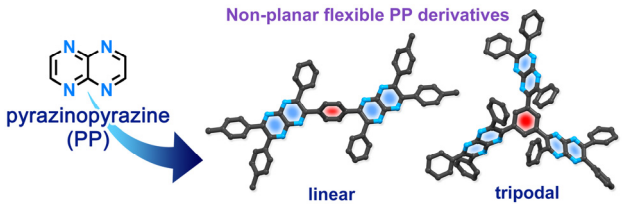

Linear and tripodal flexible π-conjugated molecules possessing two and three pyrazino[2,3-*b*]pyrazine units were synthesized. Their photophysical properties in solutions, crystal structures, and acid responsiveness are presented.

Nitrogen-containing polycyclic aromatic hydrocarbons (N-PAHs) such as pyrazinacenes have been actively investigated because of their characteristic properties including electron accepting capacity, photo-luminescence, and responsiveness against cationic species.[1] Particularly, pyrazino[2,3-*b*]pyrazine (PP) (**1**), which is a naphthalene analogue with iminium nitrogen atoms at 1,4,5,8-positions instead of sp^2-carbon atoms, is one of the simplest N-PAHs, and therefore, is attractive as a building block of nitrogen-highly-contained π-conjugated systems.[2] Tadokoro and co-workers synthesized tetraazatetracene and tetraazapentacene and showed that they can be electron acceptors that act as n-type semiconductors.[3] Richards and co-workers reported that protonation and deprotonation significantly changed the absorption spectrum of tetradecaazadihydroheptacene.[4] Bonifazi and co-workers prepared polymeric supramolecular architectures using tetraazanaphthacene and boronic acids.[5] PP-based liquid crystalline materials[6] and hydrogen-bonded organic frameworks[7] were also reported. In many systems, a PP moiety was annulated to other aromatic rings to achieve shape persistent rigid molecules with highly extended π-conjugation.

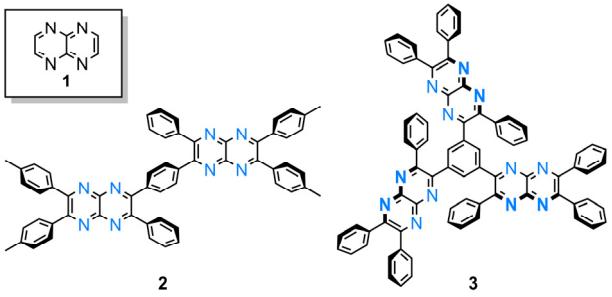

Fig. 1 Pirazinopyrazine **1** and its accumulated derivatives **2** and **3**.

In this study, on the other hand, we were interested in PP-accumulated molecules possessing flexible molecular conformation and moderate π-conjugation. Herein, we report synthesis, solution properties, crystal structures, and responses to HCl of flexible PP-accumulated π-conjugated molecules **2** and **3** (Fig. 1), in which multiple PP moieties are singly bonded to the central benzene ring. It is revealed that non-planar tripodal **3** shows blue-shifted absorption and red-shifted emission spectra compared to linear **2** that has a co-planar arrangement of two PP moieties. Moreover, **3**

forms interlocked dimers in a crystalline state. These behaviors are characteristic for flexible PP derivatives, particularly for **3**, suggesting the possibility of a new family of N-PAH compounds.

Synthesis of **2** and **3** is shown in Scheme 1. 2,3-Diamino-5,6-tolyl-pyrazinopyrazine (**6a**) was prepared by reduction of **5a**, which was synthesized by condensation of 1,2,5-thiadiazole-3,4-diamine and benzyl derivative **4a**. Similarly, **6b** was obtained according to the procedure reported in literature.[8] Diaminopyrazinopyrazine derivative **6a** was reacted with 2,2'-(1,4-phenylene)bis(1-phenylethane-1,2-dione) (**7**)[9] to give linear PP-accumulated molecule **2**. Diaminopyrazinopyrazine derivative **6b** was reacted with 2,2',2''-(benzene-1,3,5-triyl)tris(1-phenylethane-1,2-dione) (**8**)[10] to give tripodal PP-accumulated molecule **3**.

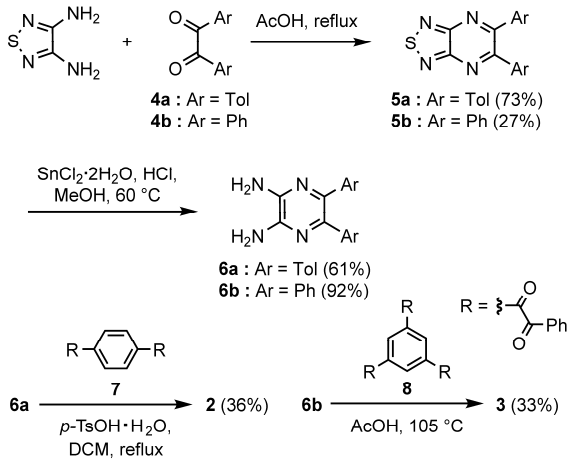

Scheme 1. Synthesis of **2** and **3**

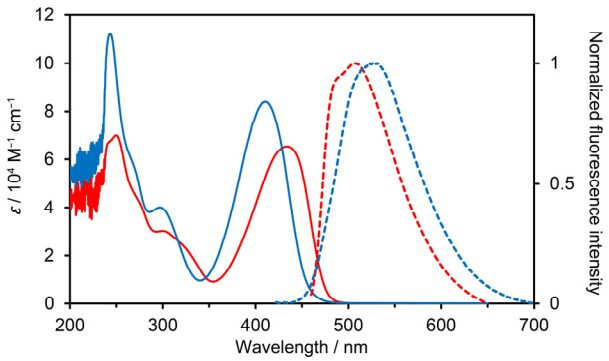

Fig. 2 Absorption (solid line) and fluorescence (dash line) spectra of linear **2** (red) and tripodal **3** (blue) in chloroform. λ_{ex} = 453 nm for **2** and 405 nm for **3**.

Fig. 2 shows UV-vis absorption and fluorescence spectra of **2** and **3** in chloroform. Linear **2** has an absorption band at 434 nm, while tripodal **3** has a band at 410 nm, which is blue-shifted by 24 nm compared to that of **2**. This difference causes from a meta-substituted skeleton and non-planar conformation of **3**, both of which prevent effective π-conjugation. Linear **2** shows a weak structureless fluorescence band at 508 nm, while **3** shows the band at 526 nm red-shifted by 18 nm compared to that of **2**. This trend of the fluorescence spectra is opposite to that of the absorption spectra. These results indicate that **3** has a more flexible molecular skeleton than **2** and is allowed to undergo conformational relaxation at the excited state. Both of **2** and **3** show very low fluorescence quantum yields (ϕ_{em} < 1%).

The redox properties of **2** and **3** were evaluated by cyclic voltammetry (CV) and differential pulse voltammetry (DPV) in THF solutions of 0.1 M *n*-Bu_4NBF_4 (Figs. S1 and S2). The CV of **2** showed two reversible overlapped reduction waves, followed by one irreversible wave. The DPV results of **2** clarified that the observed first two redox processes consisted of two successive steps (E_1= −1.51 and E_2 = −1.57 V vs Fc/Fc^+) with a very small potential splitting (ΔE = 0.06 V), indicating a weak electronic communication between the two PP moieties. Similarly, the CV of **3** showed reversible overlapped reduction waves, as well as one irreversible wave. The DPV revealed that two PP and the other PP moieties experienced one electron reduction at −1.46 and −1.61 V vs Fc/Fc^+, respectively, also indicating weak interactions among the three PP moieties in **3**.

To explore their solid-state structures, each of **2** and **3** was recrystallized by slow evaporation of chloroform/acetone mixed solutions, yielding platelet small crystals of **2** and block crystals of **3** (Fig. S3) suitable for single crystalline X-ray diffraction analysis (Table S1). Linear **2** was crystallized in the space group *P*-1 (Fig. 3). A half of the molecule is crystallographically independent, and

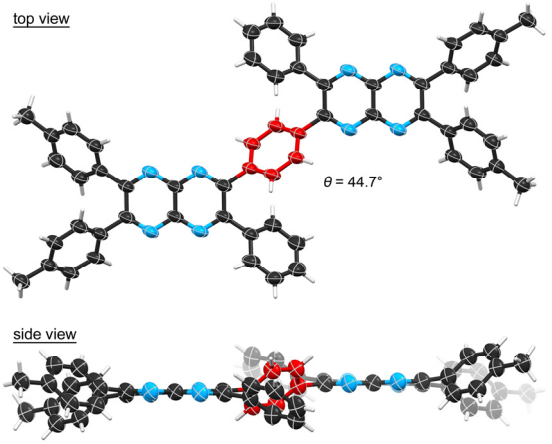

Fig. 3 Crystal structure of **2** drawn by aisotropic displacement ellipsoids with 50% probability. The central benzene ring is colored by red.

Table 1. Structural parameters for flexibility.

	$\mathbf{2}_{obs}$ [a]	$\mathbf{2}_{calc}$ [b]	$\mathbf{3}_{obs}$ [c]	$\mathbf{3}_{calc}$ [b]
θ [d] /°	44.1	37.4–42.2	42.5–54.3	38.9–43.4
ω_{in} [e] /°	35.7	37.7–42.4	40.8–76.0	39.7–44.6
ω_{out} [f] /°	17.8–48.6	37.1–41.5	24.2–85.6	37.8–42.4

[a] Molecular conformation in crystal of **2**. [b] Geometrically optimized structure calculated at CAM-B3LYP/6-311G** level of theory. [c] Molecular conformation in crystal **3**·(aceton-$CHCl_3$). [d] Dihedral angle between planes of the central benzene ring and PP moiety. [e] Dihedral angle between planes of the PP moiety and inner phenyl groups. [f] Dihedral angle between planes of the PP moiety and outer tolyl groups.

therefore, the molecule has an inversion center at the central benzene ring. Two PP groups of **2** have a nearly co-planar arrangement. The central benzene ring is twisted by 44.1° against the PP planes. The outer four tolyl groups of **2** twisted from the PP groups by 47.8°–48.6°, while the inner phenyl groups did by 35.7°. These conformational parameters are similar to these of theoretical structure optimized in vacuum (Tables 1 and S2). Because of the twisted aryl groups, π/π stacking between the PP moieties is limited, on the other hand, the PP moiety has edge-to-face contacts with the peripheral aryl groups and the central benzene ring (Fig. S4). Namely, the nitrogen atoms in the PP parts participate in formation of CH/N interactions with the phenylene group with a H···N distance of 2.58 Å and a C–H–N angle of 165.7° and CH/N interactions with the methyl groups in the peripheral toluyl groups with a N···H distance of 2.49 Å and a C–H–N angle of 156.1°. Interlayer distances of the neighboring molecules are 3.52 Å and 3.74 Å, which are longer than that of a typical π/π stacked structure (Fig. S5). The crystal structure of **2** has small, discrete voids located near by the peripheral phenyl groups and N atoms of the PP moieties (Fig. S6).

Tripodal **3** was crystallized in the space group *P*31*c*. The resultant crystal **3**·(acetone-$CHCl_3$) consists of two independent molecules (A and B) of **3** and at least one acetone and one chloroform molecules. Some of peripheral phenyl groups are crystallographically disordered because of high degree of conformational freedom (Fig. S7). The structure of **3**·(acetone-$CHCl_3$) is shown in Fig. 4. The molecules have a quasi-C_3 symmetric nonplanar conformation with *P*- or *M*-helicity. Three PP groups are twisted from the central benzene ring by 46.3° to 51.4° for molecule A (Fig. 4a) and 42.5° to 54.3° for molecule B (Table S3). Basically, molecules A and B have similar molecular conformation to each other. Dihedral angles between the inner phenyl groups and the PP groups range from 40.8° to 76.0°, which are more varied than those of theoretical structure optimized in vacuum, i.e. 39.7–44.6°, due to packing force. Similarly, dihedral angles between the outer phenyl groups and the PP groups have wide range of values from 30.7° to 85.6°.

Interestingly, tripodal molecules A and B with the same helicity form an interdigitated dimer (Fig. 4b). The staggered angle of the central benzene rings of the two molecules forming the dimer is 18.4°, although the benzene rings are not perfectly parallel. The distance between the centroids of the benzene rings is 3.94 Å. This distance is so far apart that the π-π interactions are completely negligible, while there is no enough space to encapsulate a guest molecule. This "non-utilizable" space seems to be a characteristic of the present system. The dimer structure is supported by intermolecular interactions involving the peripheral phenyl groups, such as CH/π interactions between the peripheral phenyl groups (denoted by 1, 2, 3) and CH/N interactions between and the phenyl group and PP moiety (denoted by 4). Fig. 4c shows relative orientation of three sets stacked PP moieties observed in the dimer. In these cases, the PP moieties are stacked with a center-to-center distance ranging from 3.39 Å to 3.74 Å and a staggered angle ranging from 75° to 80°. The dimers with the same helicity are then gathered with three-fold axis to give a chiral sheet structure parallel to the *ab* plane, while a neighboring sheet has the opposite chirality, resulting entirely achiral crystal structure (Fig. S8). In the crystal structure of **3**·(acetone-$CHCl_3$), trefoil-shaped inclusion spaces are connected through a narrow bottleneck, forming a two-dimensional network parallel to the *ab* plane (Fig. S9). The space includes acetone and chloroform molecules with an approximate host-guest ratio of 2:3:2 (**3**/acetone/chloroform), which was based on electron counts

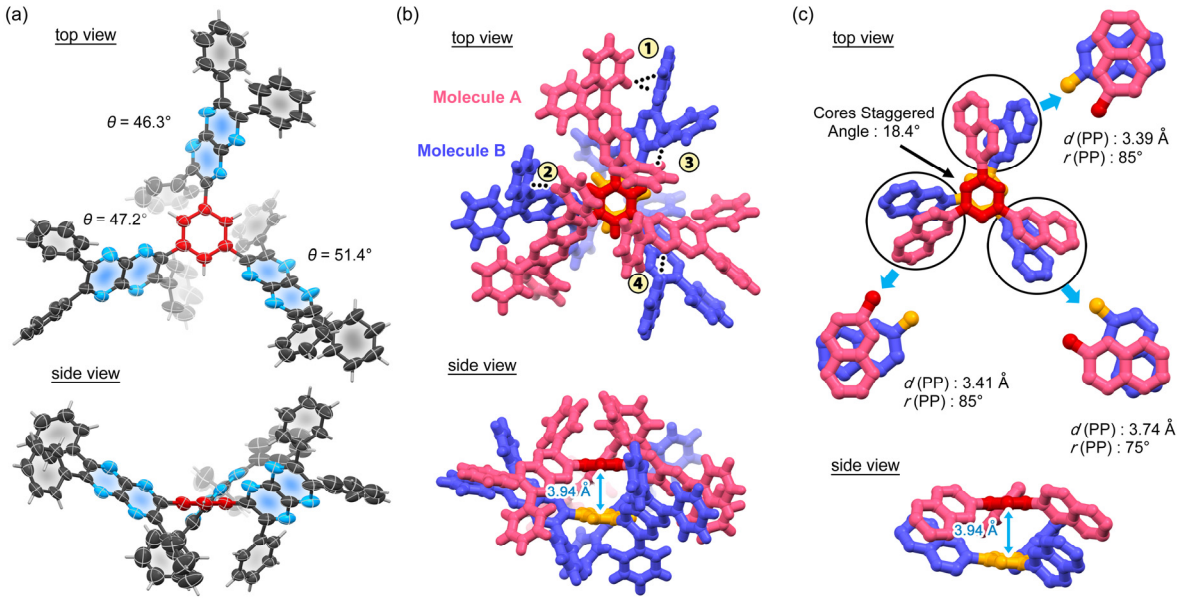

Fig. 4 Crystal structure of **3**·(aceton-$CHCl_3$). (a) Anisotropic displacement ellipsoids plot of molecule A with 50% probability from top and side of the central benzene ring (red color). (b) Interdigitated dimer composed of molecules A (pink) and B (purple), where the central benzene rings are colored by orange and red. Typical intermolecular interactions are noted by 1, 2, 3, and 4. (c) Relative orientations of the neighboring PP groups in the dimer, where *d*(PP) and *r*(PP) denote a distance and rotation angle between the stacked PP moieties, respectively.

estimated by SQEEZE process[12] and ^{1}H NMR spectrum of **3**·(acetone-$CHCl_3$) dissolved in DMSO-d_6 (Fig. S10). Thermogravimetric analysis revealed that the crystals gradually released the included solvent under ambient temperature and lost all solvent up to ca. 160 °C (Fig. S11).

Molecules containing pyrazine moieties often show acid responsiveness, as reported in several previous studies.[11] We also investigated whether **2** and **3** show acid responsiveness. Crystalline bulks of **2** and **3**·(acetone-$CHCl_3$) were exposed to hydrochloric acid vapor, resulting gradual changes of their colors from yellow to reddish yellow as a result of protonation of the PP moieties (Fig. 5). Diffuse reflectance spectra of as-formed crystals show closely similar profiles to each other. A crystalline bulk of **2** shows a new shoulder at *ca.* 550–610 nm in the spectrum with moderate intensity after the exposure. That of **3**·(acetone-$CHCl_3$) also showed red shifted band at ca. 500–580 nm. TDDFT calculations disclose that these new bands are ascribable to electron transition from neutral PP to protonated PP moieties (Figs. S12–S18). When the reddish crystals were heated or left at room temperature, they gradually returned to yellow.

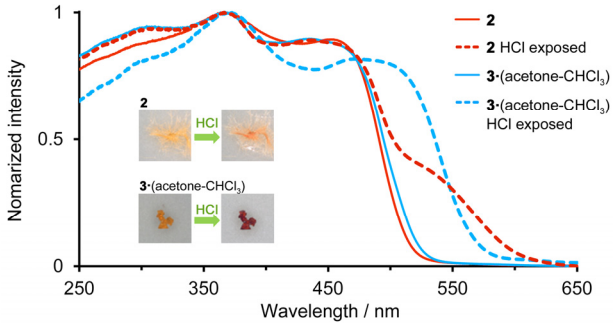

Fig. 5 Reflectance spectra of crystalline bulks of **2** and **3**·(acetone-$CHCl_3$) before and after exposed to hydrochloric acid. Inset: photographs of crystals.

In summary, we synthesized pyrazinopyrazine (PP)-based linear **2** and tripodal **3**, in which PP moieties are introduced at 1,4-positions and 1,3,5-positions of the central benzene ring, respectively, giving conformationally flexible and moderately π-conjugated molecules. Their solution properties, crystal structures, and hydrochloric acid responsiveness were revealed. Nonplanar **3** shows blue-shifted absorption and red-shifted emission spectra compared to planar **2** due to conformational flexibility of **3**. Moreover, **3** forms an unique interdigitated dimer with a small cavity in the crystalline state because of tripodal non-planar molecular shape. These PP derivatives can open a new family of N-contained π-conjugated systems.

Acknowledgement

The authors thank Dr. S. Kawamorita at Osaka University for determination of fluorescence quantum yield in solutions and Ms. R. Miyake at Osaka University for HR-MS analysis. The authors thank the Cybermedia Center, Osaka University, for use of the Super-computer for Quest to Unsolved Interdisciplinary Data science (SQUID). X-ray diffraction data of **2** was collected at BL40XU in SPring-8 with approval of JASRI (proposal Nos. 2023A1264 and 2023B1142). Dr. K. Ichiyanagi and Dr. T. Sasaki at JASRI are acknowledged for synchrotron radiation experiments.

Supplementary data

Supplementary material is available at *Chemistry Letters*

Funding

This work was supported by a Grant-in-Aid for Transformative Research Areas (A) "Condensed Conjugation" (JSPS KAKENHI Grant Number 21H05485, 23H04029, and 23H04028), and Grant-in-Aids for Scientific Research (B) (JSPS KAKENHI Grant Numbers 21H01919 and 24K01468) from the Japan Society for the Promotion of Science.

Conflict of interest statement. None declared.

References

1 a) U. H. F. Bunz, J. Freudenberg, *Acc. Chem. Res*. **2019**, *52*, 1575. b) G. J. Richards, J. P. Hill, *Acc. Chem. Res.* **2021**, *54*, 3228.

2 a) G. J. Richards, J. P. Hill, N. K. Subbaiyan, F. D'Souza, P. A. Karr, M. R. J. Elsegood, S. J. Teat, T. Mori, K. Ariga, *J. Org. Chem.* **2009**, *74*, 8914. b) Z. He, R. Mao, D. Liu, Q. Miao, *Org. Lett*. **2012**, *14*, 4190. c) J. Fleischhauer, S. Zahn, R. Beckert, U.-W. Grummt, E. Birckner, H. Gçrls, *Chem. Eur. J.* **2012**, *18*, 4549. d) K. Isoda, H. Takahashi, Y. Mutoh, N. Hoshino, T. Akutagawa, *Dalton Trans.* **2019**, *48*, 13125. e) K. Isoda, M. Matsuzaka, T. Sugaya, T. Yasuda, M. Tadokoro, *Org. Bio. Chem.* **2019**, *17*, 7884. f) K. Isoda, H. Haga, H. Kamebuchi, M. Tadokoro, *Cryst. Growth Des.* **2020**, *20*, 7081. g) Y. Yuan, K.-C. Lo, L. Szeto, W.-K. Chan, *J. Org. Chem.* **2020**, *85*, 6372. h) D. Miklík, S. F. Mousavi, Z. Burešová, A. Middleton, Y. Matsushita, J. Labuta, A. Ahsan, L. Buimaga-Iarinca, P. A. Karr, F. Bureš, G. J. Richards, P. Švec, T. Mori, K. Ariga, Y. Wakayama, C. Morari, F. D'Souza, T. A. Jung, J. P. Hill, *Commun. Chem.* **2021**, 4:29.

3 K. Isoda, M. Nakamura, T. Tatenuma, H. Ogata, T. Sugaya, M. Tadokoro, *Chem. Lett*. **2012**, *41*, 937.

4 G. J. Richards, A. Cador, S. Yamada, A. Middleton, W. A. Webre, J. Labuta, P. A. Karr, K. Ariga, F. D'Souza, S. Kahlal, J.-F. Halet, J. P. Hill, *J. Am. Chem. Soc.* **2019**, *141*, 19570.

5 I. Georgiou, S. Kervyn, A. Rossignon, F. De Leo, J. Wouters, G. Bruylants, D. Bonifazi, *J. Am. Chem. Soc.* **2017**, *139*, 2710.

6 T. Takeda, T. Ikemoto, S. Yamamoto, W. Matsuda, S. Seki, M. Mitsuishi, T. Akutagawaq, *ACS Omega* **2018**, *3*, 13694.

7 Q. Ji, K. Takahashi, S. Noro, Y. Ishigaki, K. Kokado, T. Nakamura, I. Hisaki, *Cryst. Growth Des*. **2021**, *21*, 4656.

8 a) N. Sato, H. Mizuno, *J. Chem. Res. (S)* **1977**, 250. b) N. Sato, J. Adachi, *J. Org. Chem.* **1978,** *43,* 341.

9 S. Grätz, H. Komber, M. Bauer, B. Voit, *Polym. Chem.* **2019**, *10*, 698.

10 M. Jandke, P. Strohriegl, *Macromol.* **1998**, *31*, 6434.

11 a) I. Hisaki, Y. Suzuki, E. Gomez, Q. Ji, N. Tohnai, T. Nakamura, A. Douhal, *J. Am. Chem. Soc.* **2019**, *141*, 2111. b) I. Hisaki, Q. Ji, K. Takahashi, N. Tohnai, T. Nakamura, *Cryst. Growth Des.* **2020**, *20*, 3190. c) Y. Suzuki, M. Gutiérrez, S. Tanaka, E. Gomez, N. Tohnai, N. Yasuda, N. Matubayasi, A. Douhal, I. Hisaki, *Chem. Sci.* **2021**, *12*, 9607. d) M. Kobayashi, H. Kubo, R. Oketani, I. Hisaki, *CrystEngComm*, **2022**, *24*, 5036.

12 a) P. v. d. Sluis, A. L. Spek, *Acta Crystallogr. Sect. A* **1990**, *46*, 194. b) A. L. Spek, *Acta Crystallogr. Sect. D* **2009**, *65*, 148.